Toward the continuum limit of a $(1+1)$D quantum link Schwinger model

Torsten V. Zache[1,2,3] Maarten Van Damme,[4] Jad C. Halimeh,[5] Philipp Hauke,[5] and Debasish Banerjee[6,7]

[1]*Center for Quantum Physics, University of Innsbruck, 6020 Innsbruck, Austria*
[2]*Institute for Quantum Optics and Quantum Information of the Austrian Academy of Sciences,*
6020 Innsbruck, Austria
[3]*Heidelberg University, Institut für Theoretische Physik, Philosophenweg 16, 69120 Heidelberg, Germany*
[4]*Department of Physics and Astronomy, University of Ghent, Krijgslaan 281, 9000 Gent, Belgium*
[5]*INO-CNR BEC Center and Department of Physics, University of Trento,*
Via Sommarive 14, I-38123 Trento, Italy
[6]*Saha Institute of Nuclear Physics, HBNI, 1/AF Bidhannagar, Kolkata 700064, India*
[7]*Institut für Physik, Humboldt-Universität zu Berlin, Zum Großen Windkanal 6, 12489 Berlin, Germany*

The solution of gauge theories is one of the most promising applications of quantum technologies. Here, we discuss the approach to the continuum limit for $U(1)$ gauge theories regularized via finite-dimensional Hilbert spaces of quantum spin-S operators, known as quantum link models. For quantum electrodynamics (QED) in one spatial dimension, we numerically demonstrate the continuum limit by extrapolating the ground state energy, the scalar, and the vector meson masses to large spin lengths S, large volume N, and vanishing lattice spacing a. By exactly solving Gauss's law for arbitrary S, we obtain a generalized PXP spin model and count the physical Hilbert space dimension analytically. This allows us to quantify the required resources for reliable extrapolations to the continuum limit on quantum devices. We use a functional integral approach to relate the model with large values of half-integer spins to the physics at topological angle $\Theta = \pi$. Our findings indicate that quantum devices will in the foreseeable future be able to quantitatively probe the QED regime with quantum link models.

I. INTRODUCTION

The rapid development of quantum technologies culminating in the precise control of large quantum systems [1–4] has fundamentally altered the scope of physics questions that can be addressed for strongly interacting systems. As a complementary approach to smashing nuclei in colliders to uncover their substructure, one can realize quantum many-body systems in controlled analog quantum simulators or digital quantum computers and study their ground state properties at finite density or during real-time evolution associated with quenches, which are extremely difficult to tackle using Markov chain Monte Carlo methods [5,6]. Motivated by this possibility, pioneering proposals [7–10] have been put forward to study properties of lattice gauge theories with the long-term goal of simulating quantum chromodynamics, the theory of strong interactions. These ideas have triggered an intensive theory effort to devise efficient and feasible implementations (for recent reviews

see, e.g., [11–13]), resulting in first experimental realizations [14–21] in recent years.

Nonperturbative calculations of quantum field theories (QFTs) require a careful treatment of regularization and renormalization, for which the lattice approach has proven most successful [22]. The lattice Hamiltonian of a gauge theory [23] retains exact gauge invariance, while a finite spatial lattice reduces the infinite number of degrees of freedom of the field theory to a finite number of lattice sites and links. The local Hilbert space dimension of the gauge fields, however, remains infinite in the original Wilsonian formulation. Quantum link models (QLMs) [24–26] regulate these infinite-dimensional Hilbert spaces with qudits while maintaining exact gauge invariance. They are ideal candidates to be studied on quantum devices such as analog quantum simulators or digital quantum computers, which typically work with finite-dimensional local Hilbert spaces. Extracting information relevant for the QFT in the continuum limit, especially when realized in the low-dimensional Hilbert spaces available in current quantum devices, requires a sequence of extrapolations, which is the main topic of this article.

Effects of truncating the infinite-dimensional Hilbert space have been extensively investigated for lattice theories with continuous global and local symmetries [27–36]. For

pure $U(1)$ gauge theory in $(2 + 1)$D dimensions, truncations in the magnetic basis have been argued to be superior to truncations in the electric basis for reaching the continuum limit [37] (see also [38–40]). Nevertheless, rapid convergence in such truncations has been observed previously in [41,42]. The related approach of approximating continuous groups with discrete groups of increasing order also has a long history [43–50].

The continuum limit physics is quite sensitive to the nature of the employed truncation. For example, in the $(1 + 1)$D $O(3)$ model, the physics of asymptotic freedom could only be recovered with at least a 16-dimensional local Hilbert space in the angular momentum basis truncation [51]. However, using qubit operators [52], it was shown that the same continuum limit only required two qubits per site [53]. The QLM approach is similar to this qubit regularization, but uses larger spin-S operators for the $U(1)$ gauge links. It was analytically shown that large representations for the gauge links in QLMs recover the standard Wilson lattice gauge theory [54]. A fine-tuning free approach to the continuum limit using the QLMs is via the dimensional reduction in the D-theory formulation [55]. This is, however, only possible if a phase with an exponentially large correlation length is generated [56]. In this article, we explore the former approach and show that careful analysis techniques allow us to reach the continuum limit quantitatively for certain physical observables, even with very small values of S ($\lesssim 3$–5), extending the observations made in [41,42]. We solve Gauss's law analytically for a general spin-S representation and estimate the quantum resources to simulate the continuum limit. Our results may help to improve digital quantum simulations of the massive Schwinger model [57–59], through variational quantum eigensolvers and Trotterized real-time dynamics. Finally, we use path integrals to demonstrate how large half-integer spins give rise to the topological angle $\Theta = \pi$.

II. HAMILTONIAN AND GAUSS'S LAW

We focus on $U(1)$ gauge theories in d spatial dimensions with (staggered) fermionic matter [23]. The gauge fields are described by $\hat{\mathbf{S}}_{\mathbf{n},j} = (\hat{S}^+, \hat{S}^-, \hat{S}^z)_{\mathbf{n},j}$, the raising, lowering, and z-component quantum spin-S operators on the links $(\mathbf{n}, j)$ connecting neighboring sites $\mathbf{n}$ and $\mathbf{n} + \mathbf{e}_j$ on a hypercubic lattice of size N^d.[1] For any S, the raising (lowering) operators are $S^{\pm} = (S^x \pm iS^y)/2$ with $S^{x/y}$ the x/y component of the spin vector $\vec{S}$. For the spin-$1/2$ representation, for example, the spin operators are related to Pauli matrices, $\vec{S} = \vec{\sigma}/2$. The spins are coupled to fermionic operators $\hat{\psi}_{\mathbf{n}}$ on the sites, as described by the Hamiltonian

---

[1]Throughout this work, we employ periodic boundary conditions.

$$\hat{H} = \frac{g^2}{2}\sum_{\mathbf{n},j}(\hat{S}^z_{\mathbf{n},j})^2 + \mu\sum_{\mathbf{n}}(-1)^{n_1+\cdots+n_d}\hat{\psi}^{\dagger}_{\mathbf{n}}\hat{\psi}_{\mathbf{n}} - \hat{H}_{\mathrm{m}}$$
$$- \frac{1}{2\sqrt{S(S+1)}}\sum_{\mathbf{n},j}(-1)^{\sum_{k<j}n_k}(\hat{\psi}^{\dagger}_{\mathbf{n}}\hat{S}^+_{\mathbf{n},j}\hat{\psi}_{\mathbf{n}+\mathbf{e}_j} + \mathrm{H.c.}).$$

$$(1)$$

The first two terms are the electric field energy at the bare coupling g and the staggered fermion mass μ. The gauge-matter interaction is the correlated hopping of fermions along a link with the simultaneous raising or lowering of the corresponding spin. For $d > 1$, there is the magnetic energy term, $\hat{H}_{\mathrm{m}} = \frac{1}{2g^2S^2(S+1)^2}\sum_P(\hat{S}^+_{P_1}\hat{S}^+_{P_2}\hat{S}^-_{P_3}\hat{S}^-_{P_4} + \mathrm{H.c.})$, with P labeling elementary plaquettes consisting of links $P_{1,2,3,4}$ forming a square. We identify the spins with gauge fields $(\hat{U}, \hat{U}^{\dagger}) \leftrightarrow (\hat{S}^+, \hat{S}^-)/\sqrt{S(S+1)}$ and electric field $\hat{E} \leftrightarrow \hat{S}^z$. This identification preserves the commutation relations, $[E, U^{(\dagger)}] = (-)U^{(\dagger)}$, as well as an exact gauge symmetry with $(2S + 1)$-dimensional Hilbert space. To achieve the correct scaling behavior, appropriate factors of S are inserted in the dimensionless couplings in Eq. (1) (see Sec. I in the Supplemental Material [60] for more details). The gauge transformations are generated by the Gauss law operator,

$$\hat{G}_{\mathbf{n}} = \sum_j(\hat{S}^z_{\mathbf{n}+\mathbf{e}_j,j} - \hat{S}^z_{\mathbf{n},j}) - \left[\frac{(-1)^{\mathbf{n}} - 1}{2} + \hat{\psi}^{\dagger}_{\mathbf{n}}\hat{\psi}_{\mathbf{n}}\right], \quad (2)$$

satisfying $[\hat{H}, \hat{G}_{\mathbf{n}}] = 0$. The Hilbert space thus separates into superselection sectors labeled by eigenvalues of $\hat{G}_{\mathbf{n}}$. For the physical Hilbert space $\mathcal{H}_{\mathrm{phys}}$, we require $\hat{G}_{\mathbf{n}}|\mathrm{phys}\rangle = 0$.

In the renormalization group (RG) sense, the parameters g, μ, and S can be regarded as directions in the space of couplings, to be adjusted such that the theory flows to a fixed point corresponding to the desired QFT. In the remainder of this Letter, we focus on the case of one spatial dimension, $d = 1$, where Eq. (1) provides a lattice version of the (massive) Schwinger model [61–63]. The continuum Schwinger model is parametrized by the (bare) values of the electric charge e and the fermion mass m. In its lattice version at lattice spacing a, these parameters appear through the dimensionless combinations $g = ae$ and $\mu = am$. The QFT limit is reached for large S, large N, and small a, as demonstrated in Fig. 1. Specifically, we first take the infinite spin length limit $S \to \infty$ at fixed a and N, then the thermodynamic limit $N \to \infty$ at fixed a, and finally the continuum limit $a \to 0$ at fixed μ/g. The different extrapolations have to be performed for appropriately rescaled ("renormalized") quantities that correspond to physical observables (see Sec. IV in the Supplemental Material [60] for details). In general, the final continuum limit involves a rescaling of the dimensionless coupling constants in order to reach the RG fixed point [22]. This complication
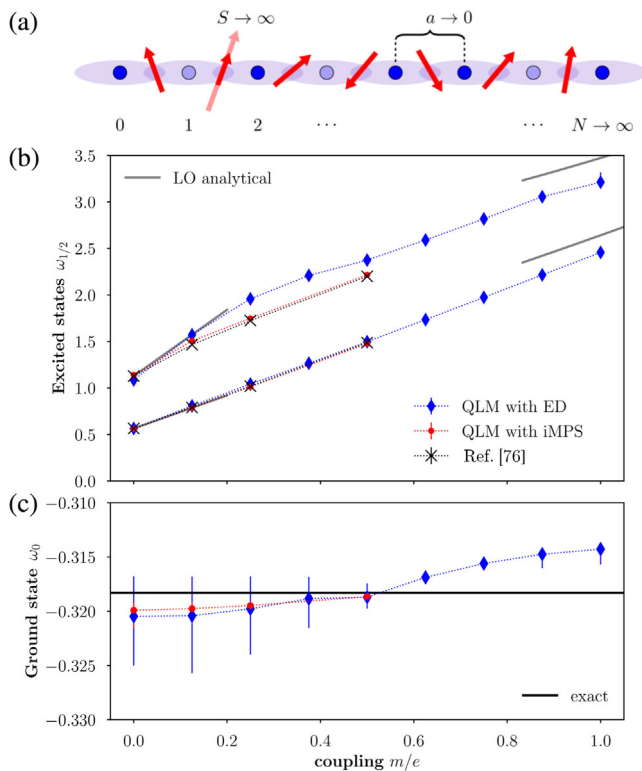
FIG. 1. (a) In a $U(1)$ QLM, matter fields (blue dots) reside on the sites of a lattice, while gauge fields, represented by spins (red arrows), live on the links connecting two neighboring lattice sites. Gauss's law ties consecutive gauge fields to the matter in between as indicated by the shaded ellipses. The ground state energy, shown in (c), and the first two excited states (with vector and scalar quantum numbers), shown in (b), in the zero momentum sector of QED obtained from the $U(1)$ QLM using ED and iMPS show excellent agreement with the analytical prediction for $m/e = 0$. In (b), the gray solid lines indicate the leading order (LO) analytical expansions [65] for small m/e and e/m, respectively. The error bars indicate an estimated systematic uncertainty (see Sec. IV in the Supplemental Material [60]).

is absent for the present model (except for a redefinition of the ground state energy) [62,64].

III. MASS SPECTRUM FROM THE QLM

The massive Schwinger model is considerably simpler than QED in higher dimensions due to the absence of magnetic interactions and the strong Gauss's law constraints. Consequently, both the weak and strong coupling limits, $e/m = 0$ and $e/m = \infty$, respectively, are exactly solvable, and analytic expansions around these limits [65,66] can be used for benchmarking the extrapolation. Our principal numerical methods are exact diagonalization (ED) (using the PYTHON package QuSpin [67]) and variational techniques based on infinite matrix product states (IMPS) [68,69] directly in the thermodynamic limit. To perform ED, we derive an equivalent spin model constrained by a projector $\mathcal{P}$ on neighboring gauge link configurations allowed by

Gauss's law. The resulting Hamiltonian has the form (see Sec. II in the Supplemental Material [60])

$$\hat{H} = \mathcal{P} \sum_{n=1}^{N} \left\{ \frac{g^2}{2} (\hat{S}_n^z)^2 + 2\mu(-1)^n \hat{S}_n^z - \frac{\hat{S}_n^x}{\sqrt{S(S+1)}} \right\} \mathcal{P}. \quad (3)$$

For $S = 1/2$, this reduces to a constrained model of hard-core bosons [70], sometimes referred to as a PXP model, whose total number of allowed states can be analytically counted [71] and which is believed to explain the anomalous thermalization observed in the 51-Rydberg atom experiment [72]. The relation between a PXP model and the spin-1/2 QLM was first noted in [73], which we generalize here to arbitrary S. Moreover, we extend the analysis of [71] and derive an analytic expression for the dimension of the physical Hilbert subspace, given by (see the Supplemental Material [60])

$$\dim \mathcal{H}_{\text{phys}}(S, N) = 2^N \sum_{m=1}^{2S+1} \left[\cos\left(\frac{m\pi}{4S+3}\right) \right]^N. \quad (4)$$

The remarkably small Hilbert space size, scaling linearly with S at a fixed N (see Sec. II in the Supplemental Material [60] for an illustration), enables ED calculations for relatively large system sizes, and data up to $S = 3$ and $N = 16$ are presented here. Results from IMPS simulations in the thermodynamic limit are also shown for $S \leq 5$ for the Hamiltonian in Eq. (1), where Gauss's law is enforced by adding a large energy penalty $\propto \sum_{\mathbf{n}} \hat{G}_{\mathbf{n}}^2$ [74,75], with $\hat{G}_{\mathbf{n}}$ defined in Eq. (2). Our results, summarized in Fig. 1, demonstrate how to accurately reach the continuum limit with QLMs for the ground state energy and the energies of the first two excited states, the "vector" and "scalar" particles. We find excellent agreement in the strong coupling limit, due to small fluctuations around $\langle \hat{S}^z \rangle = 0$, such that our numerics with small S (≤ 3 for ED and ≤ 5 for IMPS) already capture the relevant physics. For higher excited states or toward weak coupling, the fluctuations grow more pronounced and larger spin lengths S become necessary.[2]

The detailed steps of the underlying extrapolation are shown in Fig. 2 for ED, illustrated for the analytically solvable strong coupling limit ($m/e = 0$). Despite small spin lengths $S = 1, 2, 3$, we observe a clear $1/S$ scaling, enabling a reliable extrapolation to the $S \to \infty$ limit. Similarly, the subsequent $N \to \infty$ extrapolation is performed with the expected leading behavior at large N. The largest systematic error arises from the choice of fit range for the final $a \to 0$ extrapolation, which requires increasingly large values of N and S, attributed to

---

[2]The path integral construction presented in Sec. V of the Supplemental Material [60] suggests that the $U(1)$ limit can be reached by scaling the spin length as $S \propto 1/g$ for a fixed, but large, $gS \gg 1$.

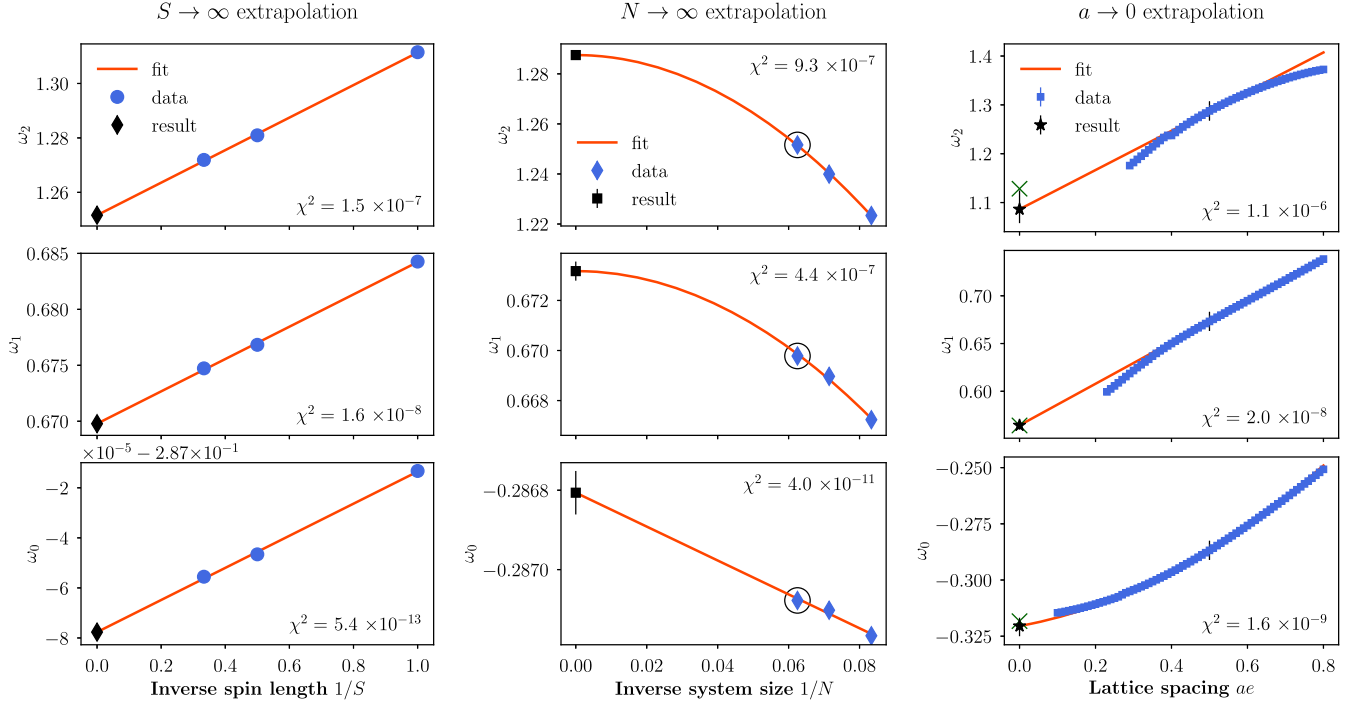FIG. 2.   We illustrate the sequence of extrapolations from left to right, required to reach the continuum limit for the ED data with $m/e = 0$. The energies of the vacuum (bottom row), vector particle (middle row), and scalar particle (top row) are extrapolated to $S \to \infty$ (left column), $N \to \infty$ (middle column), and $a \to 0$ (right column), as discussed in the main text. The circles in the middle row indicate the values obtained from the corresponding S extrapolations shown in the left column. Similarly, the ticks in the right column indicate the values corresponding to the N extrapolations in the middle column. For clarity, we only show selected values of ae and N for the first two extrapolations. For comparison, the green crosses indicate the exact analytical results. All fits employed for the extrapolations are polynomials and χ^2 denotes the resulting normalized square error of the fit (see Sec. IV of the Supplemental Material [60] for details, where we also provide a table with our quantitative results).

increasing electric field fluctuations at the continuum limit. Empirically, we find that systematic errors are minimized by disregarding "far-off" N and S extrapolation where the extrapolated values differ by more than 10% from the one of the largest available system size. We thus select a smallest lattice spacing a, for which the underlying data are sufficiently converged with respect to S and N. Note that this procedure naturally depends on the observable. The ground state energy can be extrapolated with lattice spacings down to $ae \sim 0.1$, while we only reach $ae \sim 0.3$ for the scalar mass. Details of the numerical extrapolations are presented in Sec. IV of the Supplemental Material [60].

Figure 3 shows our final results for the vector and scalar masses with a trivial m/e dependence subtracted. The IMPS results are obtained analogously to the ED simulations, but without the N extrapolation. The agreement between both approaches demonstrates that the thermodynamic limit is reached, and that the limits $S \to \infty$ and $N \to \infty$ commute for this model. Comparing to previously obtained results [76] at $S \to \infty$, we find good agreement of both the ED and IMPS data for the vector mass, indicating that $S = 3$ is sufficient to resolve this excitation. As anticipated, the scalar mass requires larger S values, and we observe stronger deviations in ED.
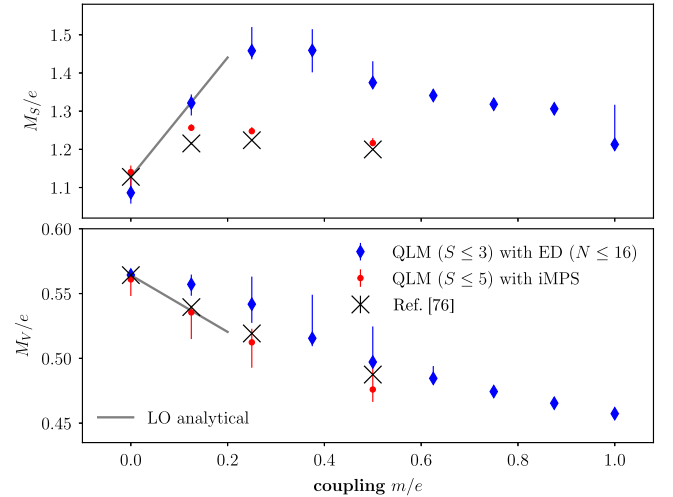

FIG. 3.   Final result for vector (lower) and scalar (upper) masses, with the leading dependence $2m/e$ subtracted. Our results reproduce the analytic prediction of the massless limit ($m/e = 0$) and are quantitatively consistent with the perturbative expectation (gray solid line). For the vector mass, both IMPS (red dots) and ED (blue diamonds) results agree with each other and previously obtained results (black crosses) at infinite spin length.

IV. ESTIMATION OF REQUIRED RESOURCES ON A QUANTUM DEVICE

As illustrated above, already very small spin lengths $S \lesssim 3$ and system sizes $N \lesssim 16$ are sufficient to obtain quantitative estimates for the low-lying mass spectrum. A brute-force implementation would nevertheless still require controlling a Hilbert space of dimension $[2(2S+1)]^N \sim 14^{16} \sim 2^{61}$. Because of Gauss's law, most of these states are unnecessary.

To estimate the minimal required resources to implement the model on a quantum device naturally working with the corresponding qudits of size $2S + 1$ [77–84], consider the equivalent spin model, Eq. (3). Then control over only $N \sim 16$ such qudits would be sufficient to reach the continuum limit. According to Eq. (4), a perfect encoding on a digital quantum computer would need only $\dim \mathcal{H}_{\text{phys}}(S = 3, N = 16) = 63757 < 2^{16}$ states, enabling our procedure to be carried out on existing quantum computing devices with control over 16 qubits. This fact has been already exploited to carry out the ED calculations on a conventional laptop computer.

To illustrate the applicability of our improved encoding [Eq. (4)], consider two examples: (i) the mass spectrum discussed above using a perfect qubit encoding and (ii) real-time dynamics on qudit hardware. The first example may be tackled with a variational quantum eigensolver (VQE) [20,85], which finds an optimal representation of an input variational ansatz for the ground or a low-lying excited state, by classically minimizing $\langle \hat{H} \rangle$. We emphasize that this does not require one to actually implement $\hat{H}$, but only to measure its expectation value. It is then favorable to work in a computational basis with the perfect encoding where $\hat{S}^z$ is diagonal, such that most terms of $\hat{H}$ can be measured directly. Only $\hat{S}^x$ has to be treated separately, which we leave for future work, but we note that it will remain local because the projection $\mathcal{P}$ acts locally. Having obtained the spectrum via VQE, the masses are extracted by classical postprocessing via the extrapolations discussed above.

For real-time dynamics, a Trotter decomposition on a system of qudits yields[3]

$$e^{-i\hat{H}\Delta t} = \prod_{n=1}^{N} e^{-i\frac{g^2}{2}(\hat{S}_n^z)^2 \Delta t} \times \prod_{n=1}^{N} e^{-i2(-1)^n \mu \hat{S}_n^z \Delta t}$$

$$\times \prod_{n=1}^{N} \mathcal{P} e^{-i/\sqrt{S(S+1)}\hat{S}_n^x \Delta t} \mathcal{P} + \mathcal{O}(\Delta t^2). \quad (5)$$

The first two single-qudit gates can be efficiently executed in parallel. For a fixed n, the off-diagonal term with $\hat{S}_n^x$

involves a projector acting locally on $(n-1, n, n+1)$. This corresponding Trotter evolution can therefore be realized as a 3-qudit controlled unitary acting only on the middle qudit n if the triplet $(n-1, n, n+1)$ is compatible with Gauss's law. This suggests to parallelize this last term in three layers, enabling scaling to large system sizes. This approach might be used, e.g., to observe the type of quench dynamics discussed in [86], where the required small spin lengths $S \leq 4$ are within reach of existing technology (see, e.g., [87] for a review of qudit quantum computing and [88] for an experimental realization, as well as [89–93] for recent related developments using qudits).

V. FIELD THEORETIC DESCRIPTION

To address the closely related question of convergence to the Kogut-Susskind limit, we use coherent state path integrals. Physically, the worldline of a spin S at spatial site $\mathbf{n}$ traces out an arbitrary closed curve on the Bloch sphere under the Hamiltonian evolution in imaginary time, subtending a solid angle Ω, as shown in Fig. 4(a). The path integral $\mathcal{Z} = \text{Tr}_{\hat{G}}(e^{-\beta \hat{H}})$ (see Sec. V of the Supplemental Material [60]) is dominated by the electric field term $(\hat{S}_{\mathbf{n}}^z)^2$, which contributes as $\sim \exp[-\epsilon g^2 S(S - 1/2)\cos^2(\theta_{\mathbf{n}})/2]$, where ϵ is the Trotter discretization and $\theta_{\mathbf{n}}, \phi_{\mathbf{n}}$ are the angular coordinates of the spin. For large $g^2 S$, $\theta_{\mathbf{n}} \to \pi/2$ as indicated in Fig. 4(b). In this limit, the quantum spin is confined to the equator of the Bloch sphere and reduces to the quantum rotor of the Wilson-Kogut-Susskind formulation, consistent with the numerics.

An important additional observation is that the area traced out by the closed curve on the Bloch sphere by $\hat{\mathbf{S}}_{\mathbf{n}}$ admits a topological interpretation as a Berry phase. In the continuum limit, this area is $\omega[\Omega] = \int_0^\beta d\tau \dot{\phi}(\tau) \cos(\theta(\phi(\tau))) = \oint_{\phi_0}^{\phi_0} d\phi \cos(\theta(\phi))$ [94], where $\tau \in [0, \beta]$ is the Euclidean time. At leading order in the large-S limit, only the number of total windings is relevant, with each winding contributing $2\pi S$. While this term is irrelevant for the integer spins used in this work, for half-integer spins it gives rise to a π flux in the system. This feature rigorously establishes that QLMs with large values of half-integer spin lead to a topological
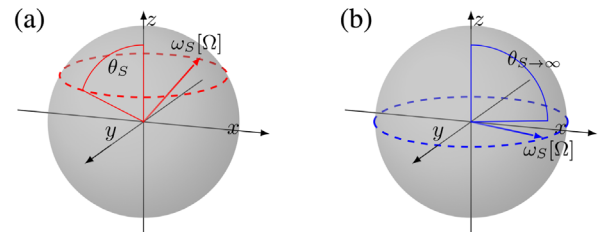

FIG. 4.   (a) Closed path traced by a quantum spin S on the Bloch sphere. (b) With increasing S, the path of the spin is forced along the equator to minimize fluctuations of the electric energy term.

---

[3]Note that here we do not enforce the perfect encoding. The Trotter decomposition is then valid on states $|\psi\rangle$ that fulfill $\mathcal{P}|\psi\rangle = |\psi\rangle$, and since $\mathcal{P}$ commutes with $\hat{S}_n^z$, the projector only appears with the terms involving $\hat{S}_n^x$.

theta angle $\Theta = \pi$, often anticipated in the literature [10,19,73,95] already for the spin-1/2 case.

VI. CONCLUSION AND OUTLOOK

In this Letter, we have numerically demonstrated the continuum limit of QED in $(1+1)$D, regularized with quantum spin-S operators for several physical observables. A highlight of our results is the small spin values $S \lesssim 3$–5 that suffice to reach the continuum limit. The systematic finite-size scaling enables us to quantitatively estimate the resources of a quantum device to realize the continuum limit. These results lend hope that near future quantum simulation experiments with small S and limited lattice size can yield valuable data that can be extrapolated to the QFT limit. Using a coherent state path integral, the approach to the Kogut-Susskind limit is derived and the connection of half-integer spins with topological angle π is formalized.

For future investigations, the feasibility of our approach may immediately be tested using today's quantum hardware. High-energy aspects of these models, such as the presence of quantum scars [96] and Floquet dynamics [97,98], are worth studying. In higher dimensions, an exciting challenge is to quantify the convergence properties of both Abelian and non-Abelian QLMs with increasing link representations. Finally, we note that the calculation of the mass spectrum of the Schwinger model using quantum devices is merely a stepping stone toward more complex tasks. The situation changes completely when considering, e.g., real-time dynamics where our proposed Trotterization using qudits can provide a substantial advantage over traditional qubit approaches.

[1] I. Bloch, J. Dalibard, and S. Nascimbène, Nat. Phys. **8**, 267 (2012).

[2] R. Blatt and C. F. Roos, Nat. Phys. **8**, 277 (2012).

[3] I. M. Georgescu, S. Ashhab, and F. Nori, Rev. Mod. Phys. **86**, 153 (2014).

[4] P. Hauke, F. M. Cucchietti, L. Tagliacozzo, I. Deutsch, and M. Lewenstein, Rep. Prog. Phys. **75**, 082401 (2012).

[5] W. Hofstetter and T. Qin, J. Phys. B **51**, 082001 (2018).

[6] U.-J. Wiese, Nucl. Phys. **A931**, 246 (2014).

[7] E. Zohar and B. Reznik, Phys. Rev. Lett. **107**, 275301 (2011).

[8] E. Zohar, J. I. Cirac, and B. Reznik, Phys. Rev. Lett. **109**, 125302 (2012).

[9] L. Tagliacozzo, A. Celi, A. Zamora, and M. Lewenstein, Ann. Phys. (Amsterdam) **330**, 160 (2013).

[10] D. Banerjee, M. Dalmonte, M. Muller, E. Rico, P. Stebler, U. J. Wiese, and P. Zoller, Phys. Rev. Lett. **109**, 175302 (2012).

[11] E. Zohar, J. I. Cirac, and B. Reznik, Rep. Prog. Phys. **79**, 014401 (2015).

[12] M. Dalmonte and S. Montangero, Contemp. Phys. **57**, 388 (2016).

[13] M. C. Banuls, R. Blatt, J. Catani, A. Celi, J. I. Cirac, M. Dalmonte, L. Fallani, K. Jansen, M. Lewenstein, S. Montangero *et al.*, Eur. Phys. J. D **74**, 165 (2020).

[14] E. A. Martinez, C. A. Muschik, P. Schindler, D. Nigg, A. Erhard, M. Heyl, P. Hauke, M. Dalmonte, T. Monz, P. Zoller *et al.*, Nature (London) **534**, 516 (2016).

[15] N. Klco, E. F. Dumitrescu, A. J. McCaskey, T. D. Morris, R. C. Pooser, M. Sanz, E. Solano, P. Lougovski, and M. J. Savage, Phys. Rev. A **98**, 032331 (2018).

[16] C. Schweizer, F. Grusdt, M. Berngruber, L. Barbiero, E. Demler, N. Goldman, I. Bloch, and M. Aidelsburger, Nat. Phys. **15**, 1168 (2019).

[17] F. Görg, K. Sandholzer, J. Minguzzi, R. Desbuquois, M. Messer, and T. Esslinger, Nat. Phys. **15**, 1161 (2019).

[18] A. Mil, T. V. Zache, A. Hegde, A. Xia, R. P. Bhatt, M. K. Oberthaler, P. Hauke, J. Berges, and F. Jendrzejewski, Science **367**, 1128 (2020).

[19] B. Yang, H. Sun, R. Ott, H.-Y. Wang, T. V. Zache, J. C. Halimeh, Z.-S. Yuan, P. Hauke, and J.-W. Pan, Nature (London) **587**, 392 (2020).

[20] Y. Atas, J. Zhang, R. Lewis, A. Jahanpour, J. F. Haase, and C. A. Muschik, Nat. Commun. **12**, 6499 (2021).

[21] H.-H. Lu, N. Klco, J. M. Lukens, T. D. Morris, A. Bansal, A. Ekström, G. Hagen, T. Papenbrock, A. M. Weiner, M. J. Savage *et al.*, Phys. Rev. A **100**, 012320 (2019).

[22] I. Montvay and G. Münster, *Quantum Fields on a Lattice* (Cambridge University Press, Cambridge, England, 1997).

[23] J. Kogut and L. Susskind, Phys. Rev. D **11**, 395 (1975).

[24] D. Horn, Phys. Lett. **100B**, 149 (1981).

[25] P. Orland and D. Rohrlich, Nucl. Phys. **B338**, 647 (1990).

[26] S. Chandrasekharan and U.-J. Wiese, Nucl. Phys. **B492**, 455 (1997).

[27] T. Byrnes, P. Sriganesh, R. J. Bursill, and C. J. Hamer, Phys. Rev. D **66**, 013002 (2002).

[28] T. Byrnes and Y. Yamamoto, Phys. Rev. A **73**, 022328 (2006).

[29] D. Yang, G. S. Giri, M. Johanning, C. Wunderlich, P. Zoller, and P. Hauke, Phys. Rev. A **94**, 052321 (2016).

[30] B. Buyens, S. Montangero, J. Haegeman, F. Verstraete, and K. Van Acoleyen, Phys. Rev. D **95**, 094509 (2017).

[31] F. Niedermayer and U. Wolff, Proc. Sci., LATTICE2016 (**2016**) 317.

[32] I. Raychowdhury and J. R. Stryker, Phys. Rev. Res. **2**, 033039 (2020).

[33] Z. Davoudi, N. M. Linke, and G. Pagano, Phys. Rev. Res. **3**, 043072 (2021).

[34] J. Unmuth-Yockey, J. Zhang, A. Bazavov, Y. Meurice, and S.-W. Tsai, Phys. Rev. D **98**, 094511 (2018).

[35] J. Zhang, Y. Meurice, and S.-W. Tsai, Phys. Rev. B **103**, 245137 (2021).

[36] E. J. Gustafson, Phys. Rev. D **103**, 114505 (2021).

[37] D. Paulson *et al.*, PRX Quantum **2**, 030334 (2021).

[38] D. B. Kaplan and J. R. Stryker, Phys. Rev. D **102**, 094515 (2020).

[39] J. F. Unmuth-Yockey, Phys. Rev. D **99**, 074502 (2019).

[40] J. Bender and E. Zohar, Phys. Rev. D **102**, 114517 (2020).

[41] S. Kühn, J. I. Cirac, and M.-C. Bañuls, Phys. Rev. A **90**, 042305 (2014).

[42] B. Buyens, S. Montangero, J. Haegeman, F. Verstraete, and K. Van Acoleyen, Phys. Rev. D **95**, 094509 (2017).

[43] G. Bhanot and C. Rebbi, Phys. Rev. D **24**, 3319 (1981).

[44] P. Hasenfratz and F. Niedermayer, Nucl. Phys. **B596**, 481 (2001).

[45] E. Ercolessi, P. Facchi, G. Magnifico, S. Pascazio, and F. V. Pepe, Phys. Rev. D **98**, 074503 (2018).

[46] A. Alexandru, P. F. Bedaque, S. Harmalkar, H. Lamm, S. Lawrence, and N. C. Warrington (NuQS Collaboration), Phys. Rev. D **100**, 114501 (2019).

[47] D. M. Kurkcuoglu, M. S. Alam, J. A. Job, A. C. Y. Li, A. Macridin, G. N. Perdue, and S. Providence, arXiv:2108 .13357.

[48] M. S. Alam, S. Hadfield, H. Lamm, and A. C. Y. Li, arXiv:2108.13305.

[49] J. Bender, E. Zohar, A. Farace, and J. I. Cirac, New J. Phys. **20**, 093001 (2018).

[50] D. C. Hackett, K. Howe, C. Hughes, W. Jay, E. T. Neil, and J. N. Simone, Phys. Rev. A **99**, 062341 (2019).

[51] F. Bruckmann, K. Jansen, and S. Kühn, Phys. Rev. D **99**, 074501 (2019).

[52] H. Singh and S. Chandrasekharan, Phys. Rev. D **100**, 054505 (2019).

[53] T. Bhattacharya, A. J. Buser, S. Chandrasekharan, R. Gupta, and H. Singh, Phys. Rev. Lett. **126**, 172001 (2021).

[54] B. Schlittgen and U. J. Wiese, Phys. Rev. D **63**, 085007 (2001).

[55] R. Brower, S. Chandrasekharan, S. Riederer, and U. J. Wiese, Nucl. Phys. **B693**, 149 (2004).

[56] B. B. Beard, M. Pepe, S. Riederer, and U. J. Wiese, Phys. Rev. Lett. **94**, 010603 (2005).

[57] A. F. Shaw, P. Lougovski, J. R. Stryker, and N. Wiebe, Quantum **4**, 306 (2020).

[58] B. Chakraborty, M. Honda, T. Izubuchi, Y. Kikuchi, and A. Tomiya, Phys. Rev. D **105**, 094503 (2022).

[59] M. Honda, E. Itou, Y. Kikuchi, L. Nagano, and T. Okuda, Phys. Rev. D **105**, 014504 (2022).

[60] See Supplemental Material at http://link.aps.org/ supplemental/10.1103/PhysRevD.106.L091502 for details about the numerical and analytical results presented in the main text.

[61] J. Schwinger, Phys. Rev. **128**, 2425 (1962).

[62] S. R. Coleman, R. Jackiw, and L. Susskind, Ann. Phys. (N.Y.) **93**, 267 (1975).

[63] S. R. Coleman, Ann. Phys. (N.Y.) **101**, 239 (1976).

[64] E. Abdalla, M. C. B. Abdalla, and K. D. Rothe, *Non-Perturbative Methods in 2 Dimensional Quantum Field Theory* (World Scientific, Singapore, 1991).

[65] P. Sriganesh, C. Hamer, and R. Bursill, Phys. Rev. D **62**, 034508 (2000).

[66] C. J. Hamer, W.-h. Zheng, and J. Oitmaa, Phys. Rev. D **56**, 55 (1997).

[67] P. Weinberg and M. Bukov, SciPost Phys. **7**, 020 (2019).

[68] V. Zauner-Stauber, L. Vanderstraeten, M. T. Fishman, F. Verstraete, and J. Haegeman, Phys. Rev. B **97**, 045145 (2018).

[69] J. Haegeman, B. Pirvu, D. J. Weir, J. I. Cirac, T. J. Osborne, H. Verschelde, and F. Verstraete, Phys. Rev. B **85**, 100408 (2012).

[70] P. Fendley, K. Sengupta, and S. Sachdev, Phys. Rev. B **69**, 075106 (2004).

[71] C. J. Turner, A. A. Michailidis, D. A. Abanin, M. Serbyn, and Z. Papić, Nat. Phys. **14**, 745 (2018).

[72] H. Bernien, S. Schwartz, A. Keesling, H. Levine, A. Omran, H. Pichler, S. Choi, A. S. Zibrov, M. Endres, M. Greiner *et al.*, Nature (London) **551**, 579 (2017).

[73] F. M. Surace, P. P. Mazza, G. Giudici, A. Lerose, A. Gambassi, and M. Dalmonte, Phys. Rev. X **10**, 021041 (2020).

[74] J. C. Halimeh and P. Hauke, Phys. Rev. Lett. **125**, 030503 (2020).

[75] M. V. Damme, J. C. Halimeh, and P. Hauke, arXiv:2010 .07338.

[76] M. C. Bañuls, K. Cichy, J. I. Cirac, and K. Jansen, J. High Energy Phys. 11 (2013) 158.

[77] V. Kasper, D. González-Cuadra, A. Hegde, A. Xia, A. Dauphin, F. Huber, E. Tiemann, M. Lewenstein, F. Jendrzejewski, and P. Hauke, Quantum Sci. Technol. **7**, 015008 (2022).

[78] Y. Wang, Z. Hu, B. C. Sanders, and S. Kais, Front. Phys. **8**, 479 (2020).

[79] E. Kiktenko, A. Fedorov, A. Strakhov, and V. Man'ko, Phys. Lett. A **379**, 1409 (2015).

[80] F. Moro, A. J. Fielding, L. Turyanska, and A. Patanè, Adv. Quantum Technol. **2**, 1900017 (2019).

[81] Y. Wang, Z. Hu, B. C. Sanders, and S. Kais, Front. Phys. **8**, 589504 (2020).

[82] S. Wang, Z.-Q. Yin, H. F. Chau, W. Chen, C. Wang, G.-C. Guo, and Z.-F. Han, Quantum Sci. Technol. **3**, 025006 (2018).

[83] B. E. Mischuck, S. T. Merkel, and I. H. Deutsch, Phys. Rev. A **85**, 022302 (2012).

[84] E. O. Kiktenko, A. S. Nikolaeva, P. Xu, G. V. Shlyapnikov, and A. K. Fedorov, Phys. Rev. A **101**, 022304 (2020).

[85] M. Cerezo, A. Arrasmith, R. Babbush, S. C. Benjamin, S. Endo, K. Fujii, J. R. McClean, K. Mitarai, X. Yuan, L. Cincio *et al.*, Nat. Rev. Phys. **3**, 625 (2021).

[86] J. C. Halimeh, M. Van Damme, T. V. Zache, D. Banerjee, and P. Hauke, arXiv:2112.04501.

[87] Y. Wang, Z. Hu, B. C. Sanders, and S. Kais, Front. Phys. **8**, 479 (2020).

[88] M. Ringbauer, M. Meth, L. Postler, R. Stricker, R. Blatt, P. Schindler, and T. Monz, Nat. Phys. **18**, 1053 (2022).

[89] A. Morvan, V. Ramasesh, M. Blok, J. Kreikebaum, K. O'Brien, L. Chen, B. Mitchell, R. Naik, D. Santiago, and I. Siddiqi, Phys. Rev. Lett. **126**, 210504 (2021).

[90] M. S. Blok, V. V. Ramasesh, T. Schuster, K. O'Brien, J.-M. Kreikebaum, D. Dahlen, A. Morvan, B. Yoshida, N. Y. Yao, and I. Siddiqi, Phys. Rev. X **11**, 021010 (2021).

[91] A. D. Hill, M. J. Hodson, N. Didier, and M. J. Reagor, arXiv:2108.01652.

[92] D. M. Kurkcuoglu, M. S. Alam, A. C. Li, A. Macridin, and G. N. Perdue, arXiv:2108.13357.

[93] M. S. Alam, S. Hadfield, H. Lamm, and A. C. Li, Phys. Rev. D **105**, 114501 (2022).

[94] M. V. Berry, Proc. R. Soc. A **392**, 45 (1984).

[95] P. Hauke, D. Marcos, M. Dalmonte, and P. Zoller, Phys. Rev. X **3**, 041018 (2013).

[96] W. W. Ho, S. Choi, H. Pichler, and M. D. Lukin, Phys. Rev. Lett. **122**, 040603 (2019).

[97] B. Mukherjee, S. Nandy, A. Sen, D. Sen, and K. Sengupta, Phys. Rev. B **101**, 245107 (2020).

[98] B. Mukherjee, A. Sen, D. Sen, and K. Sengupta, Phys. Rev. B **102**, 075123 (2020).